

A JANSKY VLA SURVEY OF MAGNETIC CATAclySMIC VARIABLE STARS: I. THE DATA

PAUL E. BARRETT^{1,2} AND CHRISTOPHER DIECK

United States Naval Observatory
 3450 Massachusetts Ave NW
 Washington, DC 20392-5420

ANTHONY J. BEASLEY

National Radio Astronomical Observatory
 520 Edgemont Road
 Charlottesville, VA 22903-2475

KULINDER P. SINGH

Tata Institute of Fundamental Research
 Dr. Homi Bhabha Road, Navy Nagar, Colaba
 Mumbai 400005, India

PAUL A. MASON

New Mexico State University
 PO Box 30001
 Las Cruces, NM 88003-8001

¹George Washington University

²paul.barrett@usno.navy.mil

ABSTRACT

The Jansky Very Large Array was used to observe 121 magnetic cataclysmic variables (MCVs). We report radio detections of 19 stars. Fourteen are new radio sources, increasing the number of MCVs that are radio sources by more than twofold, from 8 to 22. Most detections are at 8.7 GHz (X-band) with a lesser number at 5.4 and 21.1 GHz (C- and K-bands). Most flux density limits are in the range of 47–470 μ Jy. With the exception of AE Aqr, the maximum flux detected is 818 μ Jy. Fourteen of the detections show approximately 100% circularly polarized emission, which is characteristic of electron-cyclotron maser emission. The data suggest that MCVs might be divided into two classes of radio emitters: those dominated by weakly polarized gyrosynchrotron emission and those by highly polarized electron-cyclotron maser emission.

Keywords: novae, cataclysmic variables – radio continuum: stars – stars: activity – stars: magnetic fields

1. INTRODUCTION

Cataclysmic variables (CVs) are binary stars consisting of an accreting white dwarf primary and a lower main sequence, Roche-lobe filling, secondary. They are roughly divided into two classes based on their magnetic properties: systems that have a primary with a strong (> 1 MG) magnetic field, the magnetic CVs (MCVs) and those without, the normal or non-magnetic CVs.

The MCVs are further divided into two subclasses; the polars (for polarized stars), characterized by a single optical and X-ray photometric period and strong optical linear (5–10%) and circular (10–80%) polarization, and the intermediate polars (IPs) and DQ Her stars, characterized by multiple optical, and possibly X-ray, photometric periods. The magnetic field in the polars is sufficiently strong (> 10 MG) to completely disrupt the formation of an accretion disk, whereas the field in

the IPs and DQ Her stars is inferred to be weaker (1–10 MG) resulting in a truncated (inner) accretion disk. The IPs are slow rotators with $P_{\text{spin}} = 30\text{--}60$ minutes and the three DQ Her systems (DQ Her, AE Aqr, and V533 Her) are fast rotators with $P_{\text{spin}} = 30\text{--}60$ seconds, presumably caused by an episode of very high accretion similar to that of the millisecond pulsars.

Studies of CV evolution in the mid-1980s (Rappaport, Verbunt & Joss 1983, Spruit & Ritter 1983) showed that the loss of orbital angular momentum due to gravitational radiation at orbital periods > 2 h was insufficient to drive mass transfer. Another mechanism such as magnetic braking was needed. In this scenario, the outflowing stellar wind from the magnetized secondary star generates a braking torque on the binary and a loss of orbital angular momentum that is sufficiently strong to drive mass transfer at orbital periods between 3–6 h. At 3 h the secondary star becomes fully convective, which effectively turns off the magnetic braking and mass transfer. At an orbital period of about 2 h, angular momentum loss due to gravitational radiation becomes significant and mass transfer resumes. This evolutionary scenario explains the lack of CVs between two and three hours, which is called the period gap.

For MCVs, the strong magnetic field of the WD extends out to and beyond the secondary. It is therefore possible that some of the mass flow from the secondary flows out of the system along the field lines. At a WD radius of 10^{11} cm, the magnetic field of a 10 MG WD is ≈ 500 G, which equates to a cyclotron frequency of 1.4 GHz. Assuming a typical accretion rate of 10^{15} g s $^{-1}$, the radio luminosity is approximately 10^{22} ergs s $^{-1}$. Although this luminosity was well below the sensitivity of the then current radio telescopes, Chanmugan & Wagner (1978) recommended making radio observations of these systems. Based on this recommendation, R.M. Hjellming (personal communication) observed the polar AM Her (presumably using the Very Large Array), but did not detect it at a sensitivity limit of about 1 mJy, where $\text{Jy} = 10^{-26}$ W m $^{-2}$ Hz $^{-1}$.

Further observations of AM Her at 4.9 GHz using the Very Large Array (VLA) by Chanmugam & Dulk (1982) resulted in the first radio detection of a MCV. A flux density of 0.67 mJy was observed. Although the observations were made in full polarization mode, no circular polarization was observed. They concluded that the radio emission from AM Her is due to gyrosynchrotron emission (harmonic number 30–50) from energetic (≈ 350 keV) electrons trapped in the magnetosphere of the WD. EF Eri, which was also observed, was not detected at a sensitivity limit of < 0.2 mJy. They suggest that the non-detection of EF Eri might be because its magnetic field, which was not known at the time, is considerably different than AM Her; or the or-

bital separation of the stars may preclude emission at 4.9 GHz. The origin of the energetic electrons was not known, but they suggest several mechanisms for their production, such as shock waves and the unipolar inductor model of Goldreich & Lynden-Bell (1969).

Subsequent VLA observations of MCVs by Dulk, Bastian & Chanmugam (1983) again detected radio emission from AM Her at 4.9 GHz and gave upper limits at 1.4 and 15 GHz. They also obtained upper limits of about 0.2 mJy at 4.9 GHz for VV Pup, EF Eri, MR Ser, ST LMi, and AN UMa. They suggest that the quiescent emission is the result of energetic electrons (≈ 500 keV) trapped in the magnetosphere of the WD, provided that the electron energy spectrum is quite hard and the spectral hardness or number density of the energetic electrons increases with radius. Serendipitously, a radio flare lasting about 10 minutes was observed during the observation. The flare had a peak flux of 9.7 mJy (≈ 20 times the quiescent emission) and was essentially 100% circularly polarized. They concluded that the radio emission was due to an electron-cyclotron maser that operates near the surface of the red-dwarf companion in a ≈ 1 kG magnetic field. Magnetic reconnection events due to the interaction of the magnetic fields of the two stars may be the source of the energetic electrons that generate the maser emission.

The first detection of radio emission from a DQ Her binary was reported by Bookbinder & Lamb (1987) who detect strong radio emission (≈ 15 mJy at 4.9 GHz and ≈ 5 mJy at 1.4 GHz) from AE Aqr using the VLA. No radio emission was observed from five other DQ Her stars and intermediate polars (FO Aqr, AO Psc, BG CMi, TV Col, & EX Hya). They obtained upper limits of ≈ 0.2 mJy at 1.4 and 4.9 GHz. In an attempt to test the unipolar inductor model, the asynchronous polar BY Cam was observed using the VLA (Mason, Fisher, & Chanmugam, G. 1996). The upper limits obtained for this long duration VLA observation are similar to the detections of the current work. Mason & Gray (2007), during a survey of 9 MCVs at 8.4 GHz, also detected AR UMa at flux density of ≈ 0.6 mJy. AR UMa has the highest known magnetic field of all polars at 230 MG. The flux densities of two detections were 422 and 734 μ Jy. AM Her was also detected at a flux density of 584 μ Jy. The other seven targets (LW Cam, DO Dra, FIRST J1023.8+0038, SDSS J1553+5516, V2301 Oph, RX J1846.9+5538, and WZ Sge) were not detected at a flux limit of ≈ 120 μ Jy.

Bastian (1987) observed 15 MCVs, 8 polars and 7 intermediate polars and a DQ Her star, using the VLA. No detections were made at 1.5, 4.9, and 15 GHz. Beasley et al. (1994) used the Very Large Array and the Australian Telescope Compact Array to observe an additional 22 MCVs without success. However, Wright et

al. (1988) reported a detection of the polar V834 Cen at 8.4 GHz using the Parkes 64m telescope, and Pavelin, et al. (1994), observing 21 polars and IPs using the Jodrell Bank broadband interferometer, reported detections of five MCVs (BG CMi, ST LMi, DQ Her, AM Her, AE Aqr), three of which were new. For a review of the early radio observations of CVs of all types and a discussion of the radio mechanisms see Chanmugam (1987).

Since those early observations, there has been little interest in observing MCVs in the radio and hence, little progress on understanding the location and mechanism of the radio emission, because the few surveys that were done had little success. However, during the last five years, the much greater sensitivity of the Jansky Very Large Array (JVLA) has significantly improved the situation. Coppejans et al. (2015) and Coppejans et al. (2016) detected radio emission from dwarf nova and nova-like CVs at the tens of μ Jy level. For the first survey of nova-like CVs, they observed four targets and detected three of them (RW Sex, V603 Aql, and TT Ari) at 6 GHz. For the second survey of dwarf novae, they observed five targets (Z Cam, RX And, SU UMa, YZ Cnc, and U Gem) and detected all of them at flux densities between 12 and 58 μ Jy. The observed radio emission was variable on timescales of minutes to days, which is consistent with previous radio observations of other CVs.

Beginning in 2013, a project was initiated using the Very Long Baseline Array (VLBA) to perform astrometry of radio bright (> 1 mJy) MCVs in an attempt to accurately measure their distances. These results will be presented in a separate paper. At the same time, a survey was begun using the JVLA to identify any new radio bright MCVs for follow-up astrometry. The results of that survey are presented here and in a subsequent paper. The current paper presents the results of the data analysis and briefly discusses some observational statistics of the survey, while the second paper presents

a more detailed discussion of the data.

2. OBSERVATIONS AND DATA REDUCTION

We used the JVLA to observe 121 MCVs during two observing semesters, 13B and 15A, at primarily three frequencies (C-, X-, & K-bands; 4–6, 8–10 & 18–22 GHz, respectively) at full polarization. A fourth frequency, Q-band (40–44 GHz), was also used for a few observations. Accurate flux densities were obtained by observing one of four standard flux calibrators (3C48, 3C138, 3C147, and 3C286) during each scheduling block (SB), except for six SBs during semester 13B that used 3C295 as a flux calibrator and could not be accurately flux calibrated by the CASA calibration pipeline. The flux calibrators also served as linear polarization standards. However, accurate linear polarization measurements were not possible, because no polarization leakage calibrators were observed. This omission is not expected to significantly impact the measurement of circular polarization. For semester 13B, 40 h of observing time was requested to observe 60 of the optically brightest, and likely closest, MCVs. The observing program allowed about three MCVs to be observed in each one hour SB. Exposures were approximately two minutes per frequency. Each SB was scheduled twice to increase the probability of detecting the MCVs. The JVLA scheduled 35 of the 40 h, resulting in 42 MCVs being observed. For semester 15A, 69 h of observing time was requested to observe 69 MCVs. Except for one SB, each SB contained two MCVs with each exposure being approximately five minutes per frequency. The JVLA scheduled all 69 h resulting in an additional 69 MCVs being observed. These observations are summarized in Table 1. Column 1 gives the General Catalog of Variable Stars (GCVS) name. If no GCVS name is available, the star's abbreviated constellation name followed by a number is used. Column 2 is the JVLA semester–scheduling-block designation. Column 3 is the date and columns 4–9 are the UT start times and exposure lengths for the C-, X-, and K-bands, respectively.

Table 1. Log of JVLA observations

GVCS Name	Semester	C-Band		X-Band		K-Band	
		Date	Start	Expo	Start	Expo	Start
		UT	UT	(s)	UT	(s)	UT
FL Cet	13B-02A	2013-09-11	11:38:50	110	11:31:21	111	11:35:03
V1294 Tau	13B-02A	2013-09-11	11:52:25	115	11:44:09	120	11:48:18
V1309 Ori	13B-02A	2013-09-11	12:04:20	110	11:56:51	108	12:00:36
V709 Cas	13B-01A	2013-09-12	11:13:05	105	11:09:36	105	11:06:06

Table 1 continued

Table 1 (*continued*)

GVCS Name	Semester	C-Band			X-Band			K-Band		
		Date	Start	Expo	Start	Expo	Start	Expo	Start	Expo
		UT	UT	(s)	UT	(s)	UT	(s)	UT	(s)
Cas 1	13B-01A	2013-09-12	11:02:05	90	10:58:48	96	10:55:27	93		
BY Cam	13B-01A	2013-09-12	11:25:15	105	11:21:42	105	11:18:15	105		
V2301 Oph	13B-16A	2013-09-13	03:52:00	135	03:44:21	135	03:36:42	135		
V884 Her	13B-16A	2013-09-13	03:31:55	130	03:27:33	132	03:23:12	135		
V426 Oph	13B-16A	2013-09-13	03:55:20	135	03:47:39	135	03:40:00	135		
V603 Aql	13B-17A	2013-09-13	04:42:50	110	04:38:51	114	04:34:51	114		
V373 Sct	13B-17A	2013-09-13	04:55:30	115	04:51:30	114	04:47:30	114		
V1432 Aql	13B-17A	2013-09-13	05:00:10	115	05:04:06	114	05:08:06	114		
V552 Aur	13B-07A	2013-09-14	14:56:30	110	14:51:30	114	14:46:33	114		
SW Uma	13B-07A	2013-09-14	15:09:50	115	15:05:48	114	15:01:51	114		
DO Dra	13B-07A	2013-09-14	15:22:45	110	15:18:48	117	15:14:48	114		
BG Cmi	13B-09A	2013-09-14	13:25:00	120	13:21:09	114	13:17:21	117		
PQ Gem	13B-09A	2013-09-14	13:37:10	115	13:33:12	120	13:29:18	120		
Hya 1	13B-09A	2013-09-14	13:50:10	115	13:46:21	117	13:42:27	120		
AI Tri	13B-03A	2013-09-15	14:11:25	105	14:15:03	105	14:18:42	102		
TT Ari	13B-03A	2013-09-15	14:06:25	125	14:02:18	129	13:58:15	129		
GK Per	13B-03A	2013-09-15	14:31:55	125	14:27:54	123	14:23:54	126		
FL Cet	13B-02B	2013-09-16	09:02:45	110	08:55:15	111	08:58:57	111		
V1294 Tau	13B-02B	2013-09-16	09:16:20	115	09:08:03	120	09:12:12	120		
V1309 Ori	13B-02B	2013-09-16	09:28:15	110	09:20:45	108	09:24:30	111		
V603 Aql	13B-17B	2013-09-16	02:46:25	110	02:42:27	114	02:38:27	114		
V373 Sct	13B-17B	2013-09-16	02:59:05	115	02:55:06	117	02:51:06	114		
V1432 Aql	13B-17B	2013-09-16	03:03:45	115	03:07:42	114	03:11:42	114		
BY Cam	13B-06A	2013-09-17	11:15:10	115	11:11:09	117	11:07:09	117		
V405 Aur	13B-06A	2013-09-17	11:27:05	115	11:23:06	117	11:19:06	117		
MU Cam	13B-06A	2013-09-17	11:39:35	115	11:35:33	117	11:31:36	114		
BY Cam	13B-06B	2013-09-29	08:23:25	115	08:19:21	117	08:15:24	117		
V405 Aur	13B-06B	2013-09-29	08:35:20	115			08:27:21	117		
MU Cam	13B-06B	2013-09-29			08:43:48	117	08:39:48	117		
V2301 Oph	13B-16B	2013-09-29	03:14:00	135	03:06:21	138	02:58:42	138		
V884 Her	13B-16B	2013-09-29	02:53:55	135	02:49:33	138	02:45:15	135		
V426 Oph	13B-16B	2013-09-29	03:17:20	135	03:09:39	138	03:02:03	135		
V709 Cas	13B-01B	2013-10-01	09:58:20	105	09:54:51	105	09:51:21	105		
Cas 1	13B-01B	2013-10-01	09:47:20	95	09:44:00	99	09:40:42	96		
BY Cam	13B-01B	2013-10-01	10:10:30	105	10:06:57	108	10:03:27	108		
AI Tri	13B-03B	2013-10-03	07:01:35	105	07:05:12	108	07:08:54	105		
TT Ari	13B-03B	2013-10-03	06:56:35	125	06:52:30	132	06:48:27	132		
GK Per	13B-03B	2013-10-03	07:22:05	125	07:18:06	126	07:14:06	129		
QQ Vul	13B-18A	2013-10-20	01:21:15	95	01:17:03	96	01:12:54	96		
WZ Sge	13B-18A	2013-10-20	01:25:35	95	01:33:51	96	01:29:42	96		
LS Peg	13B-18A	2013-10-20	01:47:20	95	01:43:39	96	01:40:00	96		

Table 1 *continued*

Table 1 (*continued*)

GVCS Name	Semester	C-Band			X-Band			K-Band		
		Date	Start	Expo	Start	Expo	Start	Expo	Start	Expo
		UT	UT	(s)	UT	(s)	UT	(s)	UT	(s)
GI Mon	13B-08A	2013-10-22	12:55:20	120	12:51:24	120	12:47:27	123		
VV Pup	13B-08A	2013-10-22	13:07:45	120	13:03:51	120	12:59:57	120		
Hya 2	13B-08A	2013-10-22	13:20:25	115	13:16:33	117	13:12:45	117		
BG Cmi	13B-09B	2013-10-24	12:47:25	120	12:43:33	117	12:39:45	117		
PQ Gem	13B-09B	2013-10-24	12:59:30	120	12:55:36	123	12:51:42	123		
Hya 1	13B-09B	2013-10-24	13:12:35	115	13:08:45	117	13:04:51	120		
GG Leo	13B-10A	2013-10-24	13:46:05	100	13:42:39	102	13:39:09	102		
ST Lmi	13B-10A	2013-10-24	14:02:55	100	13:56:57	102	13:50:57	102		
DP Leo	13B-10A	2013-10-24	14:05:30	100	13:59:33	99	13:53:33	102		
EU Uma	13B-10A	2013-10-24	14:15:45	100	14:12:21	99	14:08:54	102		
GG Leo	13B-10B	2013-10-25	14:12:05	100	14:08:42	99	14:05:09	102		
ST Lmi	13B-10B	2013-10-25	14:29:00	100	14:22:57	102	14:17:00	102		
DP Leo	13B-10B	2013-10-25	14:31:35	100	14:25:33	102	14:19:33	102		
EU Uma	13B-10B	2013-10-25	14:41:45	100	14:38:21	102	14:34:57	102		
V552 Aur	13B-07B	2013-10-26	13:56:15	115	13:51:15	117	13:46:15	117		
SW Uma	13B-07B	2013-10-26	14:09:35	115	14:05:33	117	14:01:33	117		
DO Dra	13B-07B	2013-10-26	14:22:30	115	14:18:30	117	14:14:30	117		
GI Mon	13B-08B	2013-10-26	12:54:40	120	12:50:45	120	12:46:51	120		
VV Pup	13B-08B	2013-10-26	13:07:05	120	13:03:12	123	12:59:18	120		
Hya 2	13B-08B	2013-10-26	13:19:45	115	13:15:54	117	13:12:06	117		
TV Col	13B-05A	2013-10-27	13:07:20	125	13:03:03	132	12:58:48	132		
V348 Pup	13B-05A	2013-10-27	13:11:50	125	13:15:57	126	13:20:06	126		
V351 Pup	13B-05A	2013-10-27	13:32:55	125	13:28:45	126	13:24:36	126		
AN Uma	13B-11A	2013-10-27	14:14:20	135	14:05:48	138	13:57:21	135		
AR Uma	13B-11A	2013-10-27	14:18:10	135	14:09:39	135	14:01:09	138		
EV Uma	13B-11A	2013-10-27	14:32:40	135	14:28:00	138	14:23:21	138		
HU Aqr	13B-19A	2013-10-27	02:37:25	125	02:33:15	126	02:29:06	126		
FO Aqr	13B-19A	2013-10-27	02:50:35	125	02:46:24	126	02:42:12	129		
AO Psc	13B-19A	2013-10-27	03:03:20	125	02:59:12	126	02:55:00	129		
TV Col	13B-05B	2013-10-28	12:58:25	120	12:54:06	132	12:49:54	132		
V348 Pup	13B-05B	2013-10-28	13:02:50	125	13:07:00	126	13:11:09	126		
V351 Pup	13B-05B	2013-10-28	13:24:00	125	13:19:48	126	13:15:39	126		
AN Uma	13B-11B	2013-10-28	14:05:25	130	13:56:54	135	13:48:24	138		
AR Uma	13B-11B	2013-10-28	14:09:10	135	14:00:42	138	13:52:15	135		
EV Uma	13B-11B	2013-10-28	14:23:45	135	14:19:03	138	14:14:24	138		
QQ Vul	13B-18B	2013-11-03	03:39:25	95	03:35:15	96	03:31:06	96		
WZ Sge	13B-18B	2013-11-03	03:43:45	95	03:52:03	96	03:47:54	96		
LS Peg	13B-18B	2013-11-03	04:05:30	95	04:01:51	96	03:58:12	96		
HU Aqr	13B-19B	2013-11-06	03:42:50	125	03:38:39	126	03:34:30	126		
FO Aqr	13B-19B	2013-11-06	03:55:55	125	03:51:45	129	03:47:36	129		
AO Psc	13B-19B	2013-11-06	04:08:45	125	04:04:33	129	04:00:24	129		

Table 1 *continued*

Table 1 (*continued*)

GVCS Name	Semester	C-Band			X-Band			K-Band		
		Date	Start	Expo	Start	Expo	Start	Expo	Start	Expo
		UT	UT	(s)	UT	(s)	UT	(s)	UT	(s)
HU Aqr	13B-19B	2013-11-07	00:25:25	75	00:22:15	78	00:19:06	78		
FO Aqr	13B-19B	2013-11-07	00:38:10	75	00:34:57	78	00:31:48	78		
AO Psc	13B-19B	2013-11-07	00:50:50	75	00:47:42	75	00:44:33	75		
V795 Her	13B-15A	2013-12-02	15:53:45	125	15:49:36	126	15:45:27	126		
DQ Her	13B-15A	2013-12-02	16:06:45	125	16:02:33	126	15:58:24	126		
AM Her	13B-15A	2013-12-02	16:10:55	120	16:15:00	129	16:19:09	129		
V795 Her	13B-15B	2014-01-06	14:26:45	125	14:22:36	126	14:18:27	126		
DQ Her	13B-15B	2014-01-06	14:39:45	125	14:35:33	126	14:31:24	126		
AM Her	13B-15B	2014-01-06	14:43:55	120	14:48:00	129	14:52:09	129		
BM CrB	13B-13A	2014-01-17	13:23:25	125	13:19:12	129	13:15:03	129		
MR Ser	13B-13A	2014-01-17	13:36:50	125	13:32:42	126	13:28:33	126		
V519 Ser	13B-13A	2014-01-17	13:49:20	125	13:45:09	126	13:41:00	126		
EF Eri	13B-04A	2014-01-18	04:23:40	85	04:20:30	87	04:17:21	87		
VY For	13B-04A	2014-01-18	04:27:10	85	04:30:18	87	04:33:27	87		
AH Eri	13B-04A	2014-01-18	04:48:05	85	04:42:36	87	04:37:09	87		
IW Eri	13B-04A	2014-01-18	04:50:25	85	04:44:57	87	04:39:27	87		
EF Eri	13B-04B	2014-02-10	02:38:30	85	02:35:18	87	02:32:09	87		
VY For	13B-04B	2014-02-10	02:42:00	80	02:45:06	87	02:48:15	87		
AH Eri	13B-04B	2014-02-10	03:02:55	85	02:57:24	87	02:51:54	87		
IW Eri	13B-04B	2014-02-10	03:05:15	85	02:59:45	84	02:54:15	87		
BS Tri	15A-02A	2015-03-05	03:01:25	290	02:47:54	291	02:54:39	291		
XY Ari	15A-02A	2015-03-05	03:08:40	285	03:21:45	291	03:15:12	291		
Lyn 1	15A-14A	2015-03-06	00:51:05	280	00:38:00	282	00:44:30	285		
Cnc 2	15A-14A	2015-03-06	00:58:10	280	01:11:03	282	01:04:36	285		
LS Cam	15A-08A	2015-03-07	09:57:05	305	09:43:30	300	09:50:15	306		
HS Cam	15A-08A	2015-03-07	10:03:50	305	10:17:30	300	10:10:39	306		
FH Uma	15A-21A	2015-03-07	10:47:00	265	10:34:42	267	10:40:51	267		
EK Uma	15A-21A	2015-03-07	10:53:30	265	11:05:48	264	10:59:39	264		
V4738 Sgr	15A-35A	2015-03-07	15:53:40	115	15:46:33	114	15:50:03	117		
LW Cam	15A-10A	2015-03-08	09:10:15	305	08:56:51	300	09:03:30	306		
HT Cam	15A-10A	2015-03-08	09:17:30	305	09:31:24	303	09:24:27	306		
HY Leo	15A-20A	2015-03-08	10:01:10	290	09:48:09	285	09:54:36	294		
Leo 1	15A-20A	2015-03-08	10:06:55	290	10:20:03	285	10:13:30	291		
Sct 1	15A-27A	2015-03-08	11:11:25	290	10:58:27	291	11:04:57	291		
V1425 Aql	15A-27A	2015-03-08	11:17:05	290	11:31:00	294	11:24:03	291		
HY Leo	15A-20B	2015-03-09	07:18:40	290	07:05:36	288	07:12:06	291		
Leo 1	15A-20B	2015-03-09	07:24:25	290	07:37:33	285	07:30:57	294		
V1007 Her	15A-25A	2015-03-09	08:29:35	290	08:16:36	291	08:23:06	291		
V1323 Her	15A-25A	2015-03-09	08:36:05	290	08:49:00	294				
Mon 2	15A-11A	2015-03-10			07:18:57	291	07:25:36	291		
WX Pyx	15A-11A	2015-03-10			07:52:51	291	07:46:21	291		

Table 1 *continued*

Table 1 (*continued*)

GVCS Name	Semester	C-Band			X-Band			K-Band		
		Date	Start	Expo	Start	Expo	Start	Expo	Start	Expo
		UT	UT	(s)	UT	(s)	UT	(s)	UT	(s)
VZ Sex	15A-19A	2015-03-10	09:53:00	280	09:40:09	282	09:46:33	282		
YY Sex	15A-19A	2015-03-10	10:00:20	280	10:13:30	279	10:06:54	282		
V1007 Her	15A-25B	2015-03-10	08:33:15	290	08:20:18	291	08:26:45	291		
V1323 Her	15A-25B	2015-03-10	08:39:45	290	08:52:42	291	08:46:12	291		
V4738 Sgr	15A-35B	2015-03-15	15:52:55	115	15:45:48	111	15:49:18	117		
Vir 1	15A-22A	2015-03-28	08:43:35	310	08:29:36	309	08:36:33	312		
Vir 2	15A-22A	2015-03-28	08:49:45	305	09:03:39	312	08:56:42	309		
LW Cam	15A-10B	2015-03-31	07:54:40	305	07:41:18	300	07:47:57	306		
HT Cam	15A-10B	2015-03-31	08:01:55	305	08:15:51	303	08:08:54	306		
V1500 Cyg	15A-31A	2015-04-06	14:28:05	250	14:15:24	246	14:21:42	252		
V2069 Cyg	15A-31A	2015-04-06	14:35:50	250	14:47:57	246	14:41:54	252		
AE Aqr	15A-30A	2015-04-09	13:54:25	285	13:41:03	294	13:47:42	291		
Aqr 1	15A-30A	2015-04-09	14:00:10	285	14:13:09	285	14:06:39	288		
LS Cam	15A-08B	2015-04-10	07:46:20	305	07:32:48	303	07:39:33	306		
HS Cam	15A-08B	2015-04-10	07:53:10	305	08:06:48	300	08:00:00	306		
Tau 4	15A-05A	2015-04-12	18:57:00	310	19:10:54	318	19:03:57	315		
V1062 Tau	15A-05A	2015-04-12	18:50:35	315	18:36:06	315	18:43:18	318		
UU Col	15A-06A	2015-04-12	23:49:00	300	23:35:06	303	23:42:00	306		
Lep 1	15A-06A	2015-04-12	23:55:05	300	00:08:36	303	00:01:48	306		
V388 Peg	15A-33A	2015-04-16	15:26:10	285	15:13:21	288	15:19:45	288		
Aqr 2	15A-33A	2015-04-16	15:33:05	285	15:46:12	285	15:39:39	285		
MT Dra	15A-28A	2015-04-17	09:04:15	280	08:51:00	279	08:57:36	282		
EP Dra	15A-28A	2015-04-17	09:11:20	280	09:24:09	279	09:17:45	279		
V2731 Oph	15A-26A	2015-04-21	12:24:00	280	12:11:09	282	12:17:33	282		
Sgr 1	15A-26A	2015-04-21	12:31:25	275	12:44:00	282	12:37:42	279		
EV Lyn	15A-12A	2015-04-24	06:31:55	310	06:17:54	315	06:24:54	315		
EG Lyn	15A-12A	2015-04-24	06:38:00	315	06:51:57	318	06:45:00	315		
V388 Peg	15A-33B	2015-04-25	14:16:55	285	14:04:06	285	14:10:30	285		
Aqr 2	15A-33B	2015-04-25	14:23:50	285	14:36:54	288	14:30:21	288		
V2731 Oph	15A-26B	2015-04-28	08:20:55	280	08:08:09	282	08:14:33	282		
Sgr 1	15A-26B	2015-04-28	08:28:20	280	08:40:57	282	08:34:39	282		
V407 Vul	15A-29A	2015-04-28	14:31:05	270	14:18:39	261	14:24:48	270		
V2306 Cyg	15A-29A	2015-04-28	14:38:05	270	14:50:42	261	14:44:24	270		
AE Aqr	15A-30B	2015-04-28	13:31:45	290	13:18:27	291	13:25:06	291		
Aqr 1	15A-30B	2015-04-28	13:37:35	285	13:50:33	285	13:44:03	288		
EV Lyn	15A-12B	2015-04-29	06:16:40	315	06:02:39	318	06:09:39	318		
EG Lyn	15A-12B	2015-04-29	06:22:50	310	06:36:45	315	06:29:45	318		
Vir 1	15A-22B	2015-05-01	06:29:50	310	06:15:51	312	06:22:51	312		
Vir 2	15A-22B	2015-05-01	06:36:00	310	06:49:57	312	06:42:57	312		
V1500 Cyg	15A-31B	2015-05-01	12:51:35	250	12:38:54	246	12:45:12	252		
V2069 Cyg	15A-31B	2015-05-01	12:59:20	250	13:11:27	246	13:05:24	252		

Table 1 *continued*

Table 1 (*continued*)

GVCS Name	Semester	C-Band			X-Band			K-Band		
		Date	Start	Expo	Start	Expo	Start	Expo	Start	Expo
		UT	UT	(s)	UT	(s)	UT	(s)	UT	(s)
VZ Sex	15A-19B	2015-05-02	06:24:35	280	06:11:45	282	06:18:09	282		
YY Sex	15A-19B	2015-05-02	06:32:00	280	06:45:06	282	06:38:33	279		
IQ Eri	15A-03A	2015-05-04	16:17:50	290	16:04:45	285	16:11:12	294		
UZ For	15A-03A	2015-05-04	16:24:40	290	16:37:48	288	16:31:15	291		
AP CrB	15A-23A	2015-05-06	11:56:50	275	11:44:06	276	11:50:24	282		
V1189 Her	15A-23A	2015-05-06	12:03:10	275	12:17:12	276	12:10:06	282		
AP CrB	15A-23B	2015-05-07	12:25:50	275	12:13:06	276	12:19:24	282		
V1189 Her	15A-23B	2015-05-07	12:32:10	275	12:46:12	276	12:39:06	282		
Her 1	15A-24A	2015-05-07	04:20:30	300	04:07:15	297	04:13:48	303		
V1237 Her	15A-24A	2015-05-07	04:27:25	295	04:40:48	297	04:34:06	300		
Her 1	15A-24B	2015-05-08	04:11:25	295	03:58:09	297	04:04:42	303		
V1237 Her	15A-24B	2015-05-08	04:18:15	300	04:31:42	297	04:25:00	300		
FH Uma	15A-21B	2015-05-10	06:22:20	265	06:10:00	267	06:16:09	267		
EK Uma	15A-21B	2015-05-10	06:28:50	265	06:41:06	267	06:34:57	267		
V407 Vul	15A-29B	2015-05-10	15:12:25	265	14:59:54	261	15:06:03	270		
V2306 Cyg	15A-29B	2015-05-10	15:19:20	270	15:32:00	261	15:25:39	273		
MT Dra	15A-28B	2015-05-11	11:34:30	280	11:21:12	282	11:27:51	282		
EP Dra	15A-28B	2015-05-11	11:41:35	280	11:54:24	279	11:48:00	279		
Sct 1	15A-27B	2015-05-16	09:24:20	290	09:11:21	291	09:17:51	291		
V1425 Aql	15A-27B	2015-05-16	09:30:00	290	09:43:57	291	09:36:57	291		
Aqr 5	15A-34A	2015-05-24	14:26:50	265	14:14:39	267	14:20:45	264		
BW Scl	15A-34A	2015-05-24	14:34:35	295	14:47:48	294	14:41:09	303		
EQ Cet	15A-01A	2015-05-25	14:29:55	290	14:16:42	285	14:23:15	291		
VW For	15A-01A	2015-05-25	14:36:55	290	14:50:21	285	14:43:36	294		
Aqr 5	15A-34B	2015-05-25	13:29:40	265	13:17:33	264	13:23:36	267		
BW Scl	15A-34B	2015-05-25	13:37:25	300	13:50:42	291	13:44:03	300		
Tau 4	15A-05B	2015-05-31	14:52:15	315	15:06:12	318	14:59:15	315		
V1062 Tau	15A-05B	2015-05-31	14:45:55	310	14:31:24	315	14:38:39	315		
Aur (Paloma)	15A-07A	2015-06-01	15:05:30	280	14:51:45	285	14:58:33	291		
V647 Aur	15A-07A	2015-06-01	15:12:35	285	15:25:39	285	15:19:06	291		
Aur (Paloma)	15A-07B	2015-06-01	17:05:10	285	16:51:27	285	16:58:15	291		
V647 Aur	15A-07B	2015-06-01	17:12:20	285	17:25:21	288	17:18:48	291		
V418 Gem	15A-09A	2015-06-01	16:14:15	285	16:00:33	291	16:07:24	291		
EU Lyn	15A-09A	2015-06-01	16:20:10	290	16:33:48	291	16:27:00	291		
Mon 2	15A-11B	2015-06-03	00:38:40	290	00:25:24	291	00:32:03	291		
WX Pyx	15A-11B	2015-06-03	00:46:20	290	00:59:18	291	00:52:48	291		
EQ Cet	15A-01B	2015-06-12	13:31:40	290	13:18:27	288	13:25:00	294		
VW For	15A-01B	2015-06-12	13:38:40	290	13:52:06	288	13:45:24	291		
V418 Gem	15A-09B	2015-06-14	15:16:20	290	15:02:42	291	15:09:33	291		
EU Lyn	15A-09B	2015-06-14	15:22:20	290	15:35:57	291	15:29:09	291		
EU Cnc	15A-15A	2015-06-14	17:30:35	295	17:17:03	291	17:23:48	294		

Table 1 *continued*

Table 1 (*continued*)

GVCS Name	Semester	C-Band			X-Band			K-Band		
		Date	Start	Expo	Start	Expo	Start	Expo	Start	Expo
		UT	UT	(s)	UT	(s)	UT	(s)	UT	(s)
HS 0922+1333	15A-15A	2015-06-14	17:36:35	295	17:50:33	291	17:43:33	297		
MN Hya	15A-17A	2015-06-14	20:12:05	280	19:59:15	282	20:05:39	282		
Hya 3	15A-17A	2015-06-14	20:18:50	280	20:31:39	282	20:25:15	282		
IQ Eri	15A-03B	2015-06-15	13:17:10	290	13:04:06	285	13:10:36	291		
UZ For	15A-03B	2015-06-15	13:24:05	290	13:37:12	285	13:30:36	291		
Lyn 1	15A-14B	2015-06-28	17:33:25	280	17:20:21	282	17:26:51	285		
Cnc 2	15A-14B	2015-06-28	17:40:35	280	17:53:27	282	17:46:57	288		
DW Cnc	15A-13A	2015-07-02	15:39:25	300	15:53:03	300	15:46:12	303		
Cnc 1	15A-13A	2015-07-02	15:33:25	300	15:19:48	300	15:26:36	303		
And 1	15A-32A	2015-07-02	16:32:10	285	16:44:54	276	16:38:30	291		
Cyg 1	15A-32A	2015-07-02	16:23:45	290	16:09:30	276	16:16:30	291		
UU Col	15A-06B	2015-07-03	15:34:35	300	15:20:45	300	15:27:39	306		
Lep 1	15A-06B	2015-07-03	15:40:40	300	15:54:12	303	15:47:24	306		
And 1	15A-32B	2015-07-21	14:02:40	285	14:15:24	276	14:09:00	291		
Cyg 1	15A-32B	2015-07-21	13:54:15	290	13:40:00	276	13:47:00	291		
HY Eri	15A-04A	2015-07-25	14:22:25	280	14:09:30	282	14:15:54	285		
Mon 1	15A-04A	2015-07-25	14:30:05	275	14:43:24	282	14:36:42	285		
DW Cnc	15A-13B	2015-07-25	13:39:05	300	13:52:42	300	13:45:54	300		
Cnc 1	15A-13B	2015-07-25	13:33:05	300	13:19:27	303	13:26:15	303		
HY Eri	15A-04B	2015-07-26	13:31:20	280	13:18:24	282	13:24:48	288		
Mon 1	15A-04B	2015-07-26	13:39:00	275	13:52:18	282	13:45:36	285		
EU Cnc	15A-15B	2015-07-28	14:50:10	295	14:36:36	291	14:43:18	297		
HS 0922+1333	15A-15B	2015-07-28	14:56:10	290	15:10:06	291	15:03:06	297		
BS Tri	15A-02B	2015-08-03	14:48:10	290	14:34:42	291	14:41:27	291		
XY Ari	15A-02B	2015-08-03	14:55:25	290	15:08:33	291	15:01:57	291		
GZ Cnc	15A-16A	2015-08-06	14:43:15	290	14:29:51	288	14:36:30	291		
HU Leo	15A-16A	2015-08-06	14:49:10	290	15:02:36	288	14:55:54	291		
MN Hya	15A-17B	2015-08-21	15:49:00	280	15:36:12	282	15:42:36	282		
Hya 3	15A-17B	2015-08-21	15:55:50	280	16:08:36	282	16:02:12	282		
GZ Cnc	15A-16B	2015-09-23	11:53:00	290	11:39:39	285	11:46:18	291		
HU Leo	15A-16B	2015-09-23	11:58:55	290	12:12:24	285	12:05:39	291		
US 691	15A-18A	2015-09-27	15:10:45	255	14:58:39	258	15:04:39	261		
WX Lmi	15A-18A	2015-09-27	15:18:25	250	15:30:24	258	15:24:21	261		
US 691	15A-18B	2015-10-05	14:34:40	255	14:22:36	255	14:28:33	261		
WX Lmi	15A-18B	2015-10-05	14:42:20	250	14:54:21	255	14:48:15	261		

All data are calibrated using CASA version 4.2.2 and the JVLA calibration pipeline version 1.3.1. Although scheduling blocks 15–17 are not properly flux calibrated because CASA does not have models for the flux standard, 3C295; the flux density estimates of these data do

not appear to be grossly different compared to the properly calibrated data. Note that an incorrect flux calibration does not affect the presence of a radio source. The resulting calibrated images were then cleaned using an automated script. An image size of 2500 × 2500 pixels

was used at a scale of 0.02 arcseconds per pixel, resulting in a 50×50 arcsecond image. Six sets of uncleaned images were created; specifically, I, Q, U, V, LL, and RR. Natural weighting was used for all images. For a two minute integration, RMS errors of 25, 25, and 33 $\mu\text{Jy}/\text{beam}$ are expected for the C-, X-, and K-bands, respectively.

3. RESULTS

Table 2 lists the 121 MCVs observed during this survey and their CV subclass and optical positions. As

in Table 1, column 1 is the GCVS name. Column 2 is the CV subclass. Columns 3 and 4 are the right ascension (RA) and declination (Dec) of the star at epoch J2000. Columns 5 and 6 are the proper motion of the star, if known. Proper motions are primarily from the US Naval Observatory Combined Astrometric Catalog (UCAC4) supplemented by the Simbad on-line catalog when necessary. Columns 7 and 8 are the RA and Dec of the star at the epoch of the observation. The last two columns enable a comparison of the observed position to the catalogued position.

Table 2. Target list and their properties

GCVS Name	Class ^a	RA (hh mm ss.ss)	Dec (dd mm ss.s)	PM RA (mas)	PM Dec (mas)	RA+PM (hh mm ss.ss)	Dec+PM (dd mm ss.s)
V709 Cas	IP	00 28 48.84	+59 17 22.3	0.2	-1.8	00 28 48.84	+59 17 22.3
And 1	IP ?	00 43 08.61	+41 12 47.6	7.1	1.5	00 43 08.62	+41 12 47.6
EQ Cet	AM	01 28 52.52	-23 39 43.8	29	-34	01 28 52.55	-23 39 44.3
Cas 1	IP	01 53 20.76	+74 46 22.2			01 53 20.76	+74 46 22.2
FL Cet	AM	01 55 43.44	+00 28 06.4	64.3	13.9	01 55 43.50	+00 28 06.6
AI Tri	AM	02 03 48.60	+29 59 26.0	-8.5	-16.2	02 03 48.59	+29 59 25.8
TT Ari	VY	02 06 53.09	+15 17 41.8	-8	-24.2	02 06 53.08	+15 17 41.5
BS Tri	AM	02 09 29.80	+28 32 29.3			02 09 29.80	+28 32 29.3
VW For	AM ?	02 52 51.35	-30 37 42.6	8.6	-30.1	02 52 51.36	-30 37 43.1
IQ Eri	DN	02 55 38.03	-22 47 02.7	29	-1.9	02 55 38.06	-22 47 02.7
XY Ari	IP	02 56 08.19	+19 26 34.1			02 56 08.19	+19 26 34.1
EF Eri	AM	03 14 13.26	-22 35 43.3	123	-47	03 14 13.38	-22 35 44.0
GK Per	IP	03 31 12.01	+43 54 15.4	-8	-17.9	03 31 12.00	+43 54 15.2
VY For	AM	03 32 04.61	-25 56 55.0			03 32 04.61	-25 56 55.0
UZ For	AM	03 35 28.62	-25 44 22.3			03 35 28.62	-25 44 22.3
V1294 Tau	VY	04 00 37.23	+06 22 46.3	2.9	-4.4	04 00 37.23	+06 22 46.2
AH Eri	IP ?	04 22 38.05	-13 21 30.5			04 22 38.05	-13 21 30.5
IW Eri	AM	04 25 55.18	-19 45 30.4			04 25 55.18	-19 45 30.4
HY Eri	AM	05 01 46.39	-03 59 20.7			05 01 46.39	-03 59 20.7
V1062 Tau	IP	05 02 27.47	+24 45 23.4	-4.1	0.8	05 02 27.47	+24 45 23.4
Tau 4	AM ?	05 02 50.94	+16 24 22.0	2.9	-5	05 02 50.94	+16 24 21.9
UU Col	IP	05 12 13.22	-32 41 39.8	-2.2	11	05 12 13.22	-32 41 39.6
V1309 Ori	AM	05 15 41.41	+01 04 40.4	4.1	-8.2	05 15 41.41	+01 04 40.3
Aur (Paloma)	AM	05 24 30.48	+42 44 50.2	4.2	7	05 24 30.48	+42 44 50.3
TV Col	IP	05 29 25.52	-32 49 04.0	13.3	16.9	05 29 25.53	-32 49 03.8
BY Cam	AM	05 42 48.77	+60 51 31.5	-41	10.5	05 42 48.73	+60 51 31.6
LS Cam	IP ?	05 57 23.93	+72 41 52.6	-3.8	9.4	05 57 23.93	+72 41 52.7
V405 Aur	IP	05 57 59.27	+53 53 45.1	-2.6	-12.9	05 57 59.27	+53 53 44.9
Lep 1	AM ?	06 00 33.30	-27 09 18.5	-5	0.1	06 00 33.29	-27 09 18.5
V552 Aur	IP ?	06 14 09.81	+45 30 08.5	7.7	-7.3	06 14 09.82	+45 30 08.4
MU Cam	IP	06 25 16.18	+73 34 39.2	3.5	4.5	06 25 16.18	+73 34 39.3

Table 2 continued

Table 2 (*continued*)

GCVS Name	Class ^a	RA (hh mm ss.ss)	Dec (dd mm ss.s)	PM RA (mas)	PM Dec (mas)	RA+PM (hh mm ss.ss)	Dec+PM (dd mm ss.s)
V647 Aur	IP	06 36 32.55	+35 35 43.3	1.5	0.9	06 36 32.55	+35 35 43.3
Mon 1	AM	06 49 50.88	-07 37 41.7	6.7	8.7	06 49 50.89	-07 37 41.6
V418 Gem	IP	07 04 08.67	+26 25 10.9	1.9	1.8	07 04 08.67	+26 25 10.9
LW Cam	AM	07 04 09.98	+62 03 28.3	9.7	-12.9	07 04 09.99	+62 03 28.1
V348 Pup	SW	07 12 32.90	-36 05 38.6	1.4	8.1	07 12 32.90	-36 05 38.5
HS Cam	AM	07 19 14.49	+65 57 45.0			07 19 14.49	+65 57 45.0
GI Mon	IP ?	07 26 47.10	-06 40 29.5	7	5.4	07 26 47.11	-06 40 29.4
BG CMi	AM	07 31 29.00	+09 56 23.1	-15	-21.1	07 31 28.99	+09 56 22.8
Mon 2	AM	07 49 10.40	-05 49 25.6	-1.5	3.3	07 49 10.40	-05 49 25.5
PQ Gem	IP	07 51 17.33	+14 44 23.9	-4.3	7.7	07 51 17.33	+14 44 24.0
EU Lyn	AM	07 52 40.45	+36 28 23.2	-0.4	5.5	07 52 40.45	+36 28 23.3
EV Lyn	SW ?	07 54 43.01	+50 07 29.2	-3	-5.9	07 54 43.01	+50 07 29.1
HT Cam	IP	07 57 01.37	+63 06 01.8	-3.4	-1.1	07 57 01.37	+63 06 01.8
DW Cnc	IP	07 58 53.03	+16 16 45.2	-20.1	-3.4	07 58 53.01	+16 16 45.1
Cnc 1	AM ?	07 59 39.79	+19 14 17.3			07 59 39.79	+19 14 17.3
V351 Pup	IP ?	08 11 38.40	-35 07 30.5			08 11 38.40	-35 07 30.5
VV Pup	AM	08 15 06.78	-19 03 17.8	9.7	-70.7	08 15 06.79	-19 03 18.8
EG Lyn	AM	08 20 51.07	+49 34 31.7			08 20 51.07	+49 34 31.7
WX Pyx	IP	08 33 05.74	-22 48 32.2	-0.6	1.2	08 33 05.74	-22 48 32.2
SW UMa	SU	08 36 42.74	+53 28 38.1			08 36 42.74	+53 28 38.1
Lyn 1	AM	08 37 51.00	+38 30 12.5	-0.6	7.2	08 37 51.00	+38 30 12.6
Cnc 2	IP ?	08 46 17.12	+24 34 44.1			08 46 17.12	+24 34 44.1
EU Cnc	AM	08 51 27.19	+11 46 57.0	-13.8	-6.9	08 51 27.18	+11 46 56.9
Hya 1	AM	08 59 09.18	+05 36 54.5			08 59 09.18	+05 36 54.5
GZ Cnc	SU	09 15 51.67	+09 00 49.6	-36.4	-29.8	09 15 51.63	+09 00 49.1
HU Leo	AM ?	09 24 44.48	+08 01 51.0	6.8	-9.7	09 24 44.49	+08 01 50.8
HS 0922+1333	AM	09 24 55.94	+13 20 52.4	-17	2.6	09 24 55.92	+13 20 52.4
MN Hya	AM	09 29 07.04	-24 05 05.4	8.3	-0.9	09 29 07.05	-24 05 05.4
US 691	SU	09 32 49.57	+47 25 23.0			09 32 49.57	+47 25 23.0
VZ Sex	IP ?	09 44 31.70	+03 58 05.6	-18.3	-17.9	09 44 31.68	+03 58 05.3
HY Leo	IP	09 46 34.50	+13 50 58.1	-9	-1.5	09 46 34.49	+13 50 58.1
Leo 1	AM	09 53 08.17	+14 58 36.1			09 53 08.17	+14 58 36.1
Hya 2	AM	10 02 11.71	-19 25 37.4			10 02 11.71	-19 25 37.4
Hya 3	AM	10 07 34.64	-20 17 32.4			10 07 34.64	-20 17 32.4
GG Leo	AM	10 15 34.67	+09 04 42.0	-29.3	-8.4	10 15 34.64	+09 04 41.9
WX LMi	AM	10 26 27.49	+38 45 02.5	28	-30	10 26 27.52	+38 45 02.0
YY Sex	IP ?	10 39 46.97	-05 06 58.3	-25.7	-4	10 39 46.96	-05 00 58.1
FH UMa	AM	10 47 09.93	+63 35 13.1			10 47 09.93	+63 35 13.1
EK UMa	AM	10 51 35.15	+54 04 36.1			10 51 35.15	+54 04 36.1
AN UMa	AM	11 04 25.67	+45 03 14.0	-28.6	-17.9	11 04 25.64	+45 03 13.8
ST LMi	AM	11 05 39.76	+25 06 28.7	-1.2	-35.9	11 05 39.76	+25 06 28.2
AR UMa	AM	11 15 44.56	+42 58 22.4	-77	2	11 15 44.49	+42 58 22.4

Table 2 *continued*

Table 2 (*continued*)

GCVS Name	Class ^a	RA (hh mm ss.ss)	Dec (dd mm ss.s)	PM RA (mas)	PM Dec (mas)	RA+PM (hh mm ss.ss)	Dec+PM (dd mm ss.s)
DP Leo	AM	11 17 15.93	+17 57 42.0			11 17 15.93	+17 57 42.0
DO Dra	IP	11 43 38.50	+71 41 20.7	16.9	10.9	11 43 38.52	+71 41 20.9
EU UMa	AM	11 49 55.71	+28 45 07.6			11 49 55.71	+28 45 07.6
EV UMa	AM	13 07 53.87	+53 51 30.6			13 07 53.87	+53 51 30.6
Vir 1	AM	14 22 56.32	-02 21 08.0			14 22 56.32	-02 21 08.0
Vir 2	AM	14 24 38.93	-02 27 39.3			14 24 38.93	-02 27 39.3
BM CrB	AM	15 41 04.67	+36 02 52.9			15 41 04.67	+36 02 52.9
MR Ser	AM	15 52 47.18	+18 56 29.2	11	51.7	15 52 47.19	+18 56 29.9
AP CrB	AM	15 54 12.34	+27 21 52.4	-18	24	15 54 12.32	+27 21 52.8
V519 Ser	AM	16 10 07.51	+03 52 33.0			16 10 07.51	+03 52 33.0
Her 1	AM	16 26 08.16	+33 28 27.8			16 26 08.16	+33 28 27.8
V1189 Her	AM	16 29 36.53	+26 35 19.6	-12	-6	16 29 36.52	+26 35 19.5
V1237 Her	AM	17 00 53.30	+40 03 57.7			17 00 53.30	+40 03 57.7
V795 Her	IP	17 12 56.17	+33 31 19.2	3	-23.7	17 12 56.17	+33 31 18.9
V1007 Her	AM	17 24 06.28	+41 14 08.0	-2.4	3.2	17 24 06.28	+41 14 08.0
V2731 Oph	IP	17 30 21.90	-05 59 32.1	1	12.9	17 30 21.90	-05 59 31.9
Sgr 1	AM	17 45 32.70	-29 05 52.0	0.3	-0.6	17 45 32.70	-29 05 52.0
V2301 Oph	AM	18 00 35.58	+08 10 13.6			18 00 35.58	+08 10 13.6
V884 Her	AM	18 02 06.52	+18 04 44.9	-46.8	-75.5	18 02 06.48	+18 04 43.9
V1323 Her	IP	18 03 39.67	+40 12 20.6	1.3	-1.8	18 03 39.67	+40 12 20.6
DQ Her	IP	18 07 30.26	+45 51 32.1	5.3	16.7	18 07 30.26	+45 51 32.3
V426 Oph	IP ?	18 07 51.69	+05 51 47.8	1.7	-34.4	18 07 51.69	+05 51 47.3
AM Her	AM	18 16 13.33	+49 52 04.3	-46.3	27	18 16 13.29	+49 52 04.7
Sct 1	IP ?	18 32 20.00	-08 40 30.0	-12.1	3.8	18 32 19.99	-08 40 29.9
MT Dra	AM	18 46 58.83	+55 38 29.1	-9.9	-8.8	18 46 58.82	+55 38 29.0
V603 Aql	SH ?	18 48 54.64	+00 35 02.9	10.8	-8.7	18 48 54.65	+00 35 02.8
V373 Sct	IP ?	18 55 26.71	-07 43 05.5			18 55 26.71	-07 43 05.5
V1425 Aql	IP ?	19 05 26.68	-01 42 14.2	3.5	4.4	19 05 26.68	-01 42 14.1
EP Dra	AM	19 07 06.18	+69 08 44.2	-1.2	-10.3	19 07 06.18	+69 08 44.0
V407 Vul	AM ?	19 14 26.07	+24 56 43.3	-9.9	0.7	19 14 26.06	+24 56 43.3
V1432 Aql	AM	19 40 11.42	-10 25 25.8	-15.2	-3.5	19 40 11.41	-10 25 25.8
V2306 Cyg	IP	19 58 14.48	+32 32 42.2	0.9	2	19 58 14.48	+32 32 42.2
QQ Vul	AM	20 05 41.91	+22 39 58.9	9.2	-8.2	20 05 41.92	+22 39 58.8
WZ Sge	WZ ?	20 07 36.41	+17 42 15.4	102	-10	20 07 36.50	+17 42 15.3
V4738 Sgr	AM	20 22 37.53	-39 54 12.8			20 22 37.53	-39 54 12.8
AE Aqr	IP	20 40 09.16	-00 52 15.1	68.3	14.3	20 40 09.23	+00 52 14.9
Aqr 1	AM	20 48 27.91	+00 50 08.9	5.9	3.4	20 48 27.92	+00 50 09.0
HU Aqr	AM	21 07 58.22	-05 17 40.1	-61.9	-55.1	21 07 58.16	-05 17 40.9
V1500 Cyg	AM	21 11 36.51	+48 09 02.8	8.1	-2.6	21 11 36.52	+48 09 02.8
V2069 Cyg	IP	21 23 44.84	+42 18 01.8	-1.7	-9.6	21 23 44.84	+42 18 01.7
Cyg 1	IP	21 33 43.65	+51 07 24.5	-2	4.5	21 33 43.65	+51 07 24.6
LS Peg	IP	21 51 57.93	+14 06 53.3	17.9	-15.7	21 51 57.95	+14 06 53.1

Table 2 *continued*

Table 2 (*continued*)

GCVS Name	Class ^a	RA	Dec	PM RA	PM Dec	RA+PM	Dec+PM
		(hh mm ss.ss)	(dd mm ss.s)	(mas)	(mas)	(hh mm ss.ss)	(dd mm ss.s)
V388 Peg	AM	21 57 32.30	+08 55 15.4	-1.5	-1.6	21 57 32.30	+08 55 15.4
FO Aqr	IP	22 17 55.39	-08 21 03.8	4.1	1.6	22 17 55.39	-08 21 03.8
Aqr 2	IP ?	22 38 43.83	+01 08 20.7	-20.6	-0.3	22 38 43.81	+01 08 20.7
AO Psc	IP	22 55 17.99	-03 10 40.0	9.3	-20.5	22 55 18.00	-03 10 40.3
Aqr 5	AM	23 16 03.65	-05 27 08.7	-4.4	-18.1	23 16 03.65	-05 27 09.0
BW Scl	WZ	23 53 00.82	-38 51 46.0	74.7	-58.7	23 53 00.90	-38 51 46.9

^aThe CV subclasses are: AM = AM Herculis star (or polar), a subclass of MCVs; DN = dwarf nova; IP = intermediate polar and DQ Herculis star, subclasses of MCVs; SH = non-SU UMa star showing permanent or transient superhumps, a subclass of nova-like (NL) CVs; SU = SU Ursae Majoris star, a subtype of DN; SW = SW Sextans star, a subtype of NLs; VY = VY Sculptoris star, a subclass of NLs; WZ = WZ Sagittae star, a subclass of SU UMa stars; ? = uncertain classification.

Table 3 is the list of 19 detected MCVs. As in Table 1, columns 1 and 2 are the GCVS name and semester – scheduling-block designation. These two values uniquely determine the observation. Columns 3 and 4 are the observed source position. For stars with detections at multiple frequencies, the most accurate position is given, which equates to the measured position of the highest frequency observation. Column 5 is the distance between the observed and cataloged source positions and its standard deviation is the approximate size of the longest axis of the synthesized beam at half-width-half-maximum. Columns 6–8 are respectively the detected flux and error at the C-, X-, and K-band frequencies.

Column 9 is the significance of the detection, represented as a signal-to-noise (S/N) value. The significance of each observation is a combination of the source position and flux densities. Six of the new detections (Cas 1, BS Tri, UZ For, WX LMi, BM CrB, and Her 1) have no measured proper motion, so their cataloged position is for epoch J2000 and not for the epoch of the observation (i.e., circa J2014). This likely explains the discrepancy between the observed and catalog positions for some of these stars. As for V1007 Her, AM Her, and QQ Vul that have proper motions, we currently have no explanation for the large discrepancy in the observed and cataloged positions.

Table 3. Radio fluxes and positions of detected MCVs

GVCS Name	Semester	Observed Location		Distance ^a (arcsec)	C Flux	X Flux	K Flux	S/N	Notes ^{bc}			
		RA (hh mm ss)	Dec (dd mm ss)		Density (μJy)	Density (μJy)	Density (μJy)					
EQ Cet	15A-01A	01 28 52.633	-23 39 44.93	0.6 ± 0.2			404 ± 67	6.1	RCP			
Cas 1	13B-01A	01 53 21.091	+74 46 23.96	5.3 ± 1.6	228 ± 42			5.5	LCP, no-PM			
BS Tri	15A-02A	02 09 29.820	+28 32 28.79	0.6 ± 0.6		66 ± 21		3.4	no-PM			
EF Eri	13B-04A	03 14 13.398	-22 35 43.25	0.8 ± 1.0		352 ± 37		9.6	LCP			
UZ For	15A-03A	03 35 28.727	-25 44 22.66	0.3 ± 1.5	252 ± 24			11.7	LCP, no-PM			
Tau 4	15A-05A	05 02 50.981	+16 24 21.42	0.8 ± 0.5		250 ± 50		5.1	LCP			
VV Pup	13B-08B	08 15 06.843	-19 03 19.26	0.1 ± 0.3		161 ± 23	203 ± 29	10.5	RCP			
WX LMi	15A-18A	10 26 27.517	+38 45 02.00	0.7 ± 0.2	93 ± 15	115 ± 15		10.0	no-PM			
ST LMi	13B-10B	11 05 39.765	+25 06 28.24	0.0 ± 0.4		371 ± 46		> 50.0	LCP			
AR UMa	13B-11A	11 15 44.488	+42 58 22.41	0.0 ± 0.2	378 ± 16	420 ± 18	467 ± 35	> 50.0				

Table 3 *continued*

Table 3 (*continued*)

GVCS Name	Semester	Observed Location		Δd (arcsec)	C Flux Density (μ Jy)	X Flux Density (μ Jy)	K Flux Density (μ Jy)	S/N	Notes ^{bc}
		RA	Dec						
		(hh mm ss)	(dd mm ss)						
AR UMa	13B-11B	11 15 44.487	+42 58 22.41	0.0 ± 0.2	539 ± 22	461 ± 18	352 ± 33	> 50.0	
BM CrB	13B-13A	15 41 04.666	+36 02 52.69	0.2 ± 0.4		158 ± 28		6.1	LCP, no-PM
MR Ser	13B-13A	15 52 47.153	+18 56 29.68	0.5 ± 0.4	603 ± 35	424 ± 27		23.6	RCP
Her 1	15A-24A	16 26 08.212	+33 28 27.00	1.1 ± 0.2			218 ± 22	9.9	RCP, no-PM
V1007 Her	15A-25A	17 24 06.299	+41 14 09.97	2.0 ± 0.8		165 ± 25		6.6	RCP
V1323 Her	15A-25A	18 03 39.666	+40 12 19.61	1.0 ± 0.6		147 ± 23		6.5	LCP
V1323 Her	15A-25B	18 03 39.545	+40 12 18.71	2.8 ± 1.4	121 ± 20			6.1	RCP
AM Her	13B-15A	18 16 13.187	+49 52 05.29	1.8 ± 1.0	114 ± 12			9.5	
AM Her	13B-15B	18 16 13.186	+49 52 05.15	1.4 ± 0.4	154 ± 10	243 ± 10	818 ± 92	> 50.0	
V603 Aql	13B-17A	18 48 54.647	+00 35 02.88	0.3 ± 1.5		59 ± 19		6.0	LCP
V603 Aql	13B-17B	18 48 54.668	+00 35 03.01	0.1 ± 1.4	47 ± 8	88 ± 8		18.9	RCP
QQ Vul	13B-18B	20 05 41.901	+22 40 01.89	3.1 ± 0.2			438 ± 43	10.2	LCP
AE Aqr	15A-30A	20 40 09.231	-00 52 14.86	0.0 ± 0.2	5000 ± 22	5472 ± 18	8354 ± 38	> 50.0	
AE Aqr	15A-30B	20 40 09.233	-00 52 14.86	0.0 ± 0.2	5041 ± 20	5211 ± 16	4771 ± 30	> 50.0	

^a Δd is the distance between the observed and cataloged source positions and its standard deviation is the approximate size of the longest axis of the synthesize beam at half-width-half-maximum.

^bLCP and RCP denotes that the detection is seen in only the left-hand or right-hand circular polarization channel.

^cno-PM denotes that the source has no known proper motion. Therefore, the distance between the observed and cataloged positions may be large.

To estimate the probability that an unrelated extragalactic background radio source close to the stellar position may lead to a false detection, we use the radio source counts statistics of Condon et al. (2012). At an observing frequency of 3 GHz the number of extragalactic backgrounds sources above 100 μ Jy is approximately 1.15 million per steradian. This corresponds to an areal density of 2.7×10^{-5} per square arcsecond, i.e. the chances of an unrelated background source above 100 μ Jy being within a radius of an arcsecond of our stellar positions is extremely low, approximately 1 in 12,000. Assuming a standard spectral index for the background sources falling as spectral index $\nu^{-0.6}$, and ignoring unrelated phenomena such as interferometry resolution effects and source variability, we can also derive the chances of a confusing source within 1 arcsecond radius from the stellar positions above 100 μ Jy at 8 and 22 GHz (1 in 21,000 and 1 in 37,000, respectively).

These statistics indicate that extragalactic background sources are unlikely to contaminate our stellar radio detections. Systematic effects such as grating sidelobes from nearby sources distributing appar-

ent radio flux across our detection images, and the effects of extended thermal and non-thermal emission in some directions close to the Galactic plane, can lead to apparent radio emission from our stellar positions for some JVLA configurations. In these situations additional tests (seeking point sources, including CLEANing larger fields to remove sidelobes, comparing tentative stellar emission detections amongst different intermediate frequency and polarization channels, and developing an understanding of the regions our stellar sources are located in) can be used to develop confidence in a detection.

Table 4 lists the maximum flux density and its standard deviation for all observations, i.e., for detections and non-detections. A region having a diameter of 4 arcseconds and centered on the expected source location is used unless the observation contains a detection. In that case a background region not affected by any radio sources was used. Columns 1 and 2 are the same as those in Table 3. Columns 3–8 are the maximum flux density and its standard deviation for the C-, X-, and K-bands, respectively. For nondetections, Table 4

provides an estimate of the flux density upper limit.

Table 4. Image Statistics

GCVS Name	Semester	C Flux	X Flux	K Flux
		Density	Density	Density
		(μ Jy/beam)	(μ Jy/beam)	(μ Jy/beam)
V709 Cas	13B-01A	75 ± 35	71 ± 26	212 ± 86
V709 Cas	13B-01B	56 ± 26	52 ± 18	99 ± 34
And 1	15A-32A	26 ± 11	46 ± 12	171 ± 35
And 1	15A-32B	48 ± 14	49 ± 14	123 ± 33
EQ Cet	15A-01A	40 ± 18	30 ± 12	173 ± 36
EQ Cet	15A-01B	48 ± 14	47 ± 12	194 ± 38
Cas 1	13B-01A	104 ± 27	51 ± 19	263 ± 84
Cas 1	13B-01B	50 ± 22	54 ± 19	128 ± 38
FL Cet	13B-02A	54 ± 33	74 ± 36	329 ± 80
FL Cet	13B-02B	31 ± 16	52 ± 26	246 ± 68
AI Tri	13B-03A	113 ± 37	104 ± 27	340 ± 81
AI Tri	13B-03B	37 ± 21	54 ± 18	86 ± 30
TT Ari	13B-03A	101 ± 44	47 ± 14	188 ± 80
TT Ari	13B-03B	54 ± 24	54 ± 19	86 ± 26
BS Tri	15A-02A	48 ± 19	42 ± 14	58 ± 17
BS Tri	15A-02B	49 ± 16	47 ± 14	133 ± 32
VW For	15A-01A	27 ± 17	46 ± 19	246 ± 78
VW For	15A-01B	55 ± 18	53 ± 14	281 ± 60
IQ Eri	15A-03A	13 ± 23	50 ± 19	252 ± 75
IQ Eri	15A-03B	49 ± 16	63 ± 14	248 ± 61
XY Ari	15A-02A	42 ± 18	50 ± 15	72 ± 19
XY Ari	15A-02B	52 ± 14	44 ± 12	134 ± 30
EF Eri	13B-04A	40 ± 30	89 ± 28	110 ± 36
EF Eri	13B-04B	47 ± 21	63 ± 24	162 ± 41
GK Per	13B-03A	82 ± 42	48 ± 28	178 ± 52
GK Per	13B-03B	66 ± 31	41 ± 27	77 ± 25
VY For	13B-04A	42 ± 27	64 ± 22	146 ± 47
VY For	13B-04B	57 ± 24	61 ± 26	157 ± 40
UZ For	15A-03A	72 ± 25	65 ± 31	267 ± 91
UZ For	15A-03B	55 ± 22	52 ± 17	278 ± 93
V1294 Tau	13B-02A	67 ± 35	90 ± 37	166 ± 53
V1294 Tau	13B-02B	34 ± 21	17 ± 27	211 ± 64
AH Eri	13B-04A	48 ± 34	51 ± 22	96 ± 29
AH Eri	13B-04B	64 ± 28	65 ± 22	151 ± 41
IW Eri	13B-04A	93 ± 60	58 ± 22	127 ± 35
IW Eri	13B-04B	92 ± 40	57 ± 20	133 ± 37
HY Eri	15A-04A	565 ± 375	103 ± 32	193 ± 42
HY Eri	15A-04B	218 ± 86	146 ± 78	217 ± 56

Table 4 continued

Table 4 (*continued*)

GCVS Name	Semester	C Flux	X Flux	K Flux
		Density (μJy/beam)	Density (μJy/beam)	Density (μJy/beam)
Tau 4	15A-05A	0 ± 218	131 ± 57	94 ± 32
Tau 4	15A-05B	59 ± 79	99 ± 37	170 ± 46
V1062 Tau	15A-05A	42 ± 32	11 ± 22	90 ± 24
V1062 Tau	15A-05B	0 ± 56	52 ± 16	134 ± 42
UU Col	15A-06A	25 ± 9	36 ± 14	96 ± 34
UU Col	15A-06B	55 ± 18	38 ± 14	339 ± 93
V1309 Ori	13B-02A	100 ± 58	47 ± 16	169 ± 75
V1309 Ori	13B-02B	107 ± 63	66 ± 27	327 ± 84
Aur (Paloma)	15A-07A	40 ± 17	45 ± 15	164 ± 37
Aur (Paloma)	15A-07B	29 ± 12	46 ± 11	90 ± 26
TV Col	13B-05A	77 ± 60	107 ± 41	233 ± 96
TV Col	13B-05B	112 ± 52	94 ± 57	217 ± 70
BY Cam	13B-01A	75 ± 31	66 ± 25	333 ± 77
BY Cam	13B-06A	82 ± 32	49 ± 24	236 ± 83
BY Cam	13B-01B	38 ± 18	38 ± 18	97 ± 31
BY Cam	13B-06B	56 ± 22		96 ± 24
V405 Aur	13B-06A	340 ± 289	145 ± 67	319 ± 114
V405 Aur	13B-06B	91 ± 99		90 ± 27
LS Cam	15A-08A	40 ± 22	33 ± 11	51 ± 13
LS Cam	15A-08B	45 ± 20	31 ± 11	80 ± 23
Lep 1	15A-06A	19 ± 21	28 ± 14	132 ± 31
Lep 1	15A-06B	55 ± 19	44 ± 15	340 ± 90
V552 Aur	13B-07A	15 ± 24	63 ± 25	188 ± 66
V552 Aur	13B-07B	62 ± 23	41 ± 18	154 ± 33
MU Cam	13B-06A	75 ± 27	65 ± 22	273 ± 96
MU Cam	13B-06B			88 ± 28
V647 Aur	15A-07A	39 ± 22	47 ± 16	178 ± 49
V647 Aur	15A-07B	23 ± 19	37 ± 11	87 ± 29
Mon 1	15A-04A	64 ± 24	49 ± 15	229 ± 63
Mon 1	15A-04B	51 ± 20	48 ± 15	307 ± 86
V418 Gem	15A-09A	31 ± 15	39 ± 16	232 ± 43
V418 Gem	15A-09B	36 ± 14	33 ± 12	
LW Cam	15A-10A	23 ± 16	29 ± 13	57 ± 22
LW Cam	15A-10B	34 ± 21	43 ± 15	457 ± 141
V348 Pup	13B-05A	29 ± 25	27 ± 20	185 ± 66
V348 Pup	13B-05B	50 ± 26	68 ± 23	201 ± 67
HS Cam	15A-08A	30 ± 12	27 ± 12	59 ± 16
HS Cam	15A-08B	30 ± 12	32 ± 12	57 ± 20
GI Mon	13B-08A	53 ± 21	47 ± 17	90 ± 28
GI Mon	13B-08B	53 ± 17	56 ± 20	86 ± 29

Table 4 *continued*

Table 4 (*continued*)

GCVS Name	Semester	C Flux	X Flux	K Flux
		Density (μJy/beam)	Density (μJy/beam)	Density (μJy/beam)
BG Cmi	13B-09A	29 ± 21	23 ± 17	181 ± 81
BG Cmi	13B-09B	55 ± 17	53 ± 20	131 ± 35
Mon 2	15A-11A		51 ± 21	103 ± 27
Mon 2	15A-11B	43 ± 15	33 ± 11	93 ± 27
PQ Gem	13B-09A	41 ± 31	57 ± 24	185 ± 47
PQ Gem	13B-09B	29 ± 14	49 ± 22	125 ± 33
EU Lyn	15A-09A	34 ± 17	48 ± 11	224 ± 51
EU Lyn	15A-09B	39 ± 14	32 ± 9	
EV Lyn	15A-12A	28 ± 21	28 ± 11	69 ± 25
EV Lyn	15A-12B	21 ± 15	17 ± 9	75 ± 25
HT Cam	15A-10A	17 ± 9	33 ± 13	69 ± 22
HT Cam	15A-10B	31 ± 16	25 ± 14	89 ± 24
DW Cnc	15A-13A	57 ± 26	46 ± 16	204 ± 59
DW Cnc	15A-13B	66 ± 27	51 ± 19	270 ± 72
Cnc 1	15A-13A	41 ± 15	52 ± 16	235 ± 60
Cnc 1	15A-13B	53 ± 16	44 ± 15	405 ± 88
V351 Pup	13B-05A	45 ± 22	60 ± 21	150 ± 54
V351 Pup	13B-05B	33 ± 17	43 ± 20	154 ± 48
VV Pup	13B-08A	60 ± 23	58 ± 26	159 ± 36
VV Pup	13B-08B	78 ± 33	44 ± 21	114 ± 35
EG Lyn	15A-12A	22 ± 12	34 ± 12	63 ± 23
EG Lyn	15A-12B	42 ± 16	28 ± 12	73 ± 21
WX Pyx	15A-11A		46 ± 17	162 ± 42
WX Pyx	15A-11B	46 ± 13	57 ± 13	141 ± 43
SW Uma	13B-07A	0 ± 38	51 ± 28	141 ± 50
SW Uma	13B-07B	47 ± 17	48 ± 15	102 ± 31
Lyn 1	15A-14A	26 ± 16	50 ± 19	63 ± 16
Lyn 1	15A-14B	48 ± 14	32 ± 10	139 ± 31
Cnc 2	15A-14A	24 ± 17	43 ± 19	54 ± 15
Cnc 2	15A-14B	40 ± 13	36 ± 12	130 ± 31
EU Cnc	15A-15A	40 ± 13	60 ± 15	262 ± 62
EU Cnc	15A-15B	39 ± 21	48 ± 15	249 ± 79
Hya 1	13B-09A	182 ± 93	50 ± 29	216 ± 78
Hya 1	13B-09B	39 ± 44	55 ± 27	127 ± 36
GZ Cnc	15A-16A	61 ± 21	53 ± 15	212 ± 60
GZ Cnc	15A-16B	40 ± 14	56 ± 16	251 ± 67
HU Leo	15A-16A	45 ± 14	52 ± 16	192 ± 52
HU Leo	15A-16B	44 ± 14	47 ± 13	210 ± 54
HS 0922+1333	15A-15A	36 ± 15	30 ± 14	314 ± 79
HS 0922+1333	15A-15B	44 ± 16	31 ± 16	289 ± 80

Table 4 continued

Table 4 (*continued*)

GCVS Name	Semester	C Flux	X Flux	K Flux
		Density (μJy/beam)	Density (μJy/beam)	Density (μJy/beam)
MN Hya	15A-17A	58 ± 18	51 ± 15	274 ± 78
MN Hya	15A-17B	47 ± 19	42 ± 15	336 ± 71
US 691	15A-18A	28 ± 13	43 ± 13	65 ± 46
VZ Sex	15A-19A	16 ± 12	41 ± 12	68 ± 26
VZ Sex	15A-19B	23 ± 26	36 ± 15	101 ± 37
HY Leo	15A-20A	60 ± 31	42 ± 11	92 ± 24
HY Leo	15A-20B	42 ± 17	45 ± 15	79 ± 19
Leo 1	15A-20A	48 ± 23	40 ± 14	87 ± 24
Leo 1	15A-20B	33 ± 14	45 ± 13	74 ± 18
Hya 2	13B-08A	20 ± 41	61 ± 22	144 ± 41
Hya 2	13B-08B	17 ± 33	37 ± 22	127 ± 40
Hya 3	15A-17A	28 ± 33	70 ± 22	372 ± 87
Hya 3	15A-17B	47 ± 23	63 ± 25	262 ± 76
GG Leo	13B-10A	63 ± 26	70 ± 26	112 ± 41
GG Leo	13B-10B	66 ± 25	61 ± 22	175 ± 45
WX Lmi	15A-18A	91 ± 17	90 ± 17	133 ± 37
YY Sex	15A-19A	18 ± 17	35 ± 16	87 ± 24
YY Sex	15A-19B	7 ± 19	32 ± 17	108 ± 33
FH Uma	15A-21A	37 ± 14	34 ± 14	72 ± 18
FH Uma	15A-21B	30 ± 15	28 ± 11	84 ± 20
EK Uma	15A-21A	47 ± 16	34 ± 13	61 ± 16
EK Uma	15A-21B	42 ± 10	29 ± 11	61 ± 19
AN Uma	13B-11A	40 ± 19	61 ± 20	117 ± 32
AN Uma	13B-11B	63 ± 23	50 ± 16	122 ± 37
ST Lmi	13B-10A	48 ± 24	89 ± 38	134 ± 37
ST Lmi	13B-10B	50 ± 23	51 ± 17	146 ± 39
AR Uma	13B-11A	378 ± 16	420 ± 18	467 ± 35
AR Uma	13B-11B	539 ± 22	461 ± 18	352 ± 33
DP Leo	13B-10A	89 ± 34	61 ± 25	143 ± 41
DP Leo	13B-10B	55 ± 29	50 ± 21	139 ± 47
DO Dra	13B-07A	54 ± 22	38 ± 17	308 ± 70
DO Dra	13B-07B	47 ± 28	44 ± 14	103 ± 33
EU Uma	13B-10A	78 ± 41	78 ± 26	146 ± 43
EU Uma	13B-10B	99 ± 42	63 ± 29	197 ± 47
EV Uma	13B-11A	44 ± 15	57 ± 18	92 ± 39
EV Uma	13B-11B	52 ± 21	47 ± 18	107 ± 36
Vir 1	15A-22A	28 ± 10	29 ± 10	64 ± 17
Vir 1	15A-22B	33 ± 21	38 ± 16	94 ± 23
Vir 2	15A-22A	42 ± 23	33 ± 13	48 ± 14
Vir 2	15A-22B	76 ± 25	39 ± 15	79 ± 22

Table 4 *continued*

Table 4 (*continued*)

GCVS Name	Semester	C Flux	X Flux	K Flux
		Density (μJy/beam)	Density (μJy/beam)	Density (μJy/beam)
BM CrB	13B-13A	62 ± 28	67 ± 22	72 ± 25
MR Ser	13B-13A	274 ± 23	164 ± 18	100 ± 24
AP CrB	15A-23A	20 ± 69	40 ± 11	86 ± 29
AP CrB	15A-23B	0 ± 81	34 ± 16	97 ± 25
V519 Ser	13B-13A	36 ± 16	43 ± 17	88 ± 28
Her 1	15A-24A	40 ± 13	29 ± 10	89 ± 24
Her 1	15A-24B	45 ± 21	30 ± 13	73 ± 20
V1189 Her	15A-23A	667 ± 347	1144 ± 402	113 ± 97
V1189 Her	15A-23B	597 ± 241	1032 ± 417	270 ± 82
V1237 Her	15A-24A	40 ± 18	33 ± 12	79 ± 25
V1237 Her	15A-24B	59 ± 33	34 ± 12	61 ± 21
V795 Her	13B-15A	9 ± 5	115 ± 48	
V795 Her	13B-15B	14 ± 8	26 ± 10	357 ± 105
V1007 Her	15A-25A	32 ± 15	35 ± 16	83 ± 25
V1007 Her	15A-25B	28 ± 12	29 ± 11	69 ± 22
V2731 Oph	15A-26A	371 ± 160	357 ± 141	213 ± 63
V2731 Oph	15A-26B	67 ± 110	255 ± 148	220 ± 78
Sgr 1	15A-26A	3900 ± 2940	0 ± 432	3 ± 119
Sgr 1	15A-26B	3453 ± 2046	0 ± 348	66 ± 120
V2301 Oph	13B-16A	21 ± 9	40 ± 16	
V2301 Oph	13B-16B	23 ± 15	60 ± 19	1300 ± 507
V884 Her	13B-16A	43 ± 24	41 ± 16	
V884 Her	13B-16B	42 ± 20	78 ± 26	1426 ± 447
V1323 Her	15A-25A	42 ± 18	50 ± 21	
V1323 Her	15A-25B	29 ± 11	29 ± 11	102 ± 21
V426 Oph	13B-16A	369 ± 154	146 ± 102	
V426 Oph	13B-16B	121 ± 99	148 ± 61	1060 ± 610
DQ Her	13B-15A	41 ± 7	128 ± 50	
DQ Her	13B-15B	23 ± 12	37 ± 14	288 ± 104
AM Her	13B-15A	70 ± 6	162 ± 52	
AM Her	13B-15B	104 ± 6	198 ± 14	665 ± 98
Sct 1	15A-27A	229 ± 175	15 ± 15	79 ± 29
Set 1	15A-27B	76 ± 36	45 ± 15	80 ± 22
MT Dra	15A-28A	27 ± 17	22 ± 10	55 ± 18
MT Dra	15A-28B	37 ± 20	31 ± 12	56 ± 18
V603 Aql	13B-17A	20 ± 8	44 ± 17	
V603 Aql	13B-17B	29 ± 5	57 ± 12	292 ± 104
V373 Sct	13B-17A	14 ± 8	50 ± 14	
V373 Sct	13B-17B	25 ± 12	24 ± 9	429 ± 119
V1425 Aql	15A-27A	55 ± 23	34 ± 16	134 ± 42

Table 4 continued

Table 4 (*continued*)

GCVS Name	Semester	C Flux	X Flux	K Flux
		Density (μJy/beam)	Density (μJy/beam)	Density (μJy/beam)
V1425 Aql	15A-27B	40 ± 15	38 ± 11	104 ± 22
EP Dra	15A-28A	23 ± 16	23 ± 11	57 ± 17
EP Dra	15A-28B	20 ± 9	31 ± 14	71 ± 18
V407 Vul	15A-29A	30 ± 18	30 ± 12	77 ± 23
V407 Vul	15A-29B	77 ± 36	33 ± 13	69 ± 23
V1432 Aql	13B-17A	9 ± 5	32 ± 12	
V1432 Aql	13B-17B	9 ± 7	26 ± 6	472 ± 145
V2306 Cyg	15A-29A	22 ± 12	44 ± 15	62 ± 23
V2306 Cyg	15A-29B	28 ± 12	31 ± 14	55 ± 18
QQ Vul	13B-18A	76 ± 34	92 ± 31	147 ± 56
QQ Vul	13B-18B	36 ± 34	40 ± 17	119 ± 35
WZ Sge	13B-18A	129 ± 45	76 ± 36	147 ± 48
WZ Sge	13B-18B	63 ± 30	62 ± 26	161 ± 44
V4738 Sgr	15A-35A	45 ± 27	99 ± 35	195 ± 55
V4738 Sgr	15A-35B	37 ± 19	68 ± 37	143 ± 49
AE Aqr	15A-30A	47 ± 22	51 ± 18	120 ± 38
AE Aqr	15A-30B	36 ± 20	61 ± 16	96 ± 30
Aqr 1	15A-30A	16 ± 13	39 ± 14	47 ± 16
Aqr 1	15A-30B	41 ± 17	41 ± 15	80 ± 21
HU Aqr	13B-19A	248 ± 59	179 ± 77	176 ± 55
HU Aqr	13B-19B			186 ± 46
V1500 Cyg	15A-31A	14 ± 13	37 ± 14	53 ± 18
V1500 Cyg	15A-31B	3 ± 23	39 ± 14	72 ± 26
V2069 Cyg	15A-31A	34 ± 12	42 ± 14	67 ± 18
V2069 Cyg	15A-31B	36 ± 16	25 ± 11	82 ± 22
Cyg 1	15A-32A	56 ± 15	39 ± 14	218 ± 56
Cyg 1	15A-32B	57 ± 19	46 ± 13	146 ± 41
LS Peg	13B-18A	77 ± 30	59 ± 25	114 ± 37
LS Peg	13B-18B	76 ± 31	69 ± 24	115 ± 37
V388 Peg	15A-33A	59 ± 22	46 ± 15	55 ± 16
V388 Peg	15A-33B	32 ± 14	26 ± 10	71 ± 19
FO Aqr	13B-19A	46 ± 19	62 ± 22	126 ± 36
FO Aqr	13B-19B	40 ± 20	46 ± 19	96 ± 29
Aqr 2	15A-33A	38 ± 17	39 ± 13	64 ± 16
Aqr 2	15A-33B	37 ± 14	28 ± 13	64 ± 22
AO Psc	13B-19A	87 ± 25	69 ± 34	117 ± 41
AO Psc	13B-19B	73 ± 29	62 ± 23	107 ± 31
Aqr 5	15A-34A	44 ± 13	40 ± 11	64 ± 18
Aqr 5	15A-34B	23 ± 13	36 ± 13	93 ± 23
BW Scl	15A-34A	42 ± 16	30 ± 14	111 ± 36

Table 4 *continued*

Table 4 (*continued*)

GCVS Name	Semester	C Flux	X Flux	K Flux
		Density ($\mu\text{Jy}/\text{beam}$)	Density ($\mu\text{Jy}/\text{beam}$)	Density ($\mu\text{Jy}/\text{beam}$)
BW Scl	15A-34B	34 ± 16	30 ± 10	142 ± 44
HU Aqr	13B-19C	70 ± 43	198 ± 82	214 ± 55
HU Aqr	13B-19D	206 ± 76	191 ± 91	143 ± 45
FO Aqr	13B-19C	72 ± 30	77 ± 27	177 ± 54
FO Aqr	13B-19D	81 ± 31	99 ± 29	136 ± 43
AO Psc	13B-19C	39 ± 46	78 ± 37	153 ± 54
AO Psc	13B-19D	85 ± 42	57 ± 24	146 ± 47

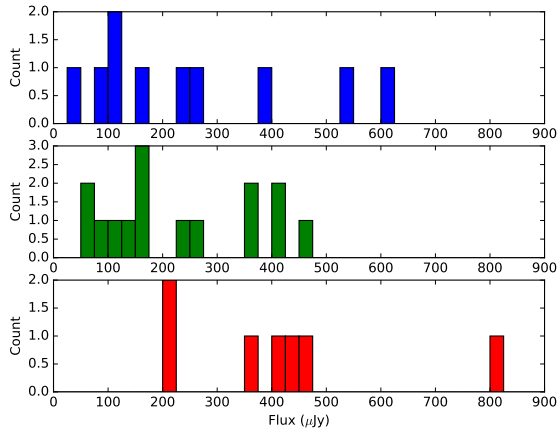


Figure 1. Flux histograms. From top to bottom, the panels are the C-band, X-band, and K-band flux densities, respectively. The flux densities of AE Aqr, being $> 5 \text{ mJy}$, are excluded.

4. DISCUSSION

There are currently eleven known CVs that are radio sources: four are polars, AM Her, AR UMa, ST LMi, and V834 Cen; four are IPs or DQ Her stars, AE Aqr, BG CMi, DQ Her, and GK Per; and three are considered non-magnetic CVs: RW Sex, TT Ari, and V603 Aql, which are classified as dwarf novae or nova-likes. This survey increases the number of CVs that are radio sources to 25. The significance of all detections except one (BS Tri) are ($> 5\sigma$). This result is a twofold increase in the number of CVs that are radio sources. Fifteen of the new detections are polars; three are IPs, and one is a non-magnetic CV.

The radio fluxes of most detections are in the range 47–470 μJy , except for AE Aqr, AM Her, AR UMa, and MR Ser (see Figure 1). AE Aqr and AR UMa show radio emission at all frequencies (C-, X-, & K-bands) and at both epochs. Whereas AM Her shows emission

at all frequencies at only a single epoch. The remaining sixteen sources show emission at no more than two frequencies. All CVs show variable emission at some level, even the three strong sources; AE Aqr, AM Her, and AR UMa. The variability of the radio flux at different epochs and frequencies is characteristic of short timescale flares. For example, the polar AM Her shows faint (114 μJy) C-band emission during the first observation on 2013-12-02 and moderate emission (154, 243, & 818 μJy) at three frequencies (C, X, & K, respectively) during the second observation 34 days later on 2014-01-06.

The small sample (19) of detections limits the comparison of the frequency dependence of the radio emission to two subclasses, polars and non-polars. For the polars, the number of detections at the C-, X-, and K-bands are 7, 12, and 7, respectively. For the non-polars with the exclusion of AE Aqr, the numbers are respectively 3, 3, and 0. This suggests that the polars are more likely to emit at higher frequencies ($> 22 \text{ GHz}$) compared to the non-polars. We note that, except for AE Aqr, these observations are the first detections of polars at 22 GHz.

A notable feature of Table 3 is the fourteen detections that show essentially 100% circularly polarized emission (i.e., a source is only seen in the left-hand or right-hand circular polarization image), whereas the remaining five detections show no (linear and circularly) polarized emission. In addition the timescale of the emission is short, < 5 minutes. These two properties are characteristic of electron-cyclotron maser emission like that of the ten minute flare of AM Her. Four of these sources show polarized emission at 22 GHz. The other five radio sources show no (or weakly) polarized emission. Three of them are the well-known MCVs, AM Her, AR UMa, and AE Aqr. These results suggest that MCVs might

be divided into two classes of radio emitters: emission dominated by weakly polarized gyrosynchrotron radiation and by highly polarized electron-cyclotron maser emission.

5. CONCLUSIONS

The current survey indicates that MCVs are highly variable radio sources that can emit at frequencies as high as 22 GHz via gyrosynchrotron and electron-cyclotron maser emission. The data suggest that the polars are more likely to emit at higher frequencies than the non-polars, and MCVs can be divided into two classes of radio emitters: those dominated by weakly polarized gyrosynchrotron emission and those by highly polarized electron-cyclotron maser emission.

Paper two of this survey presents a more in-depth analysis of these data by investigating the two radiation mechanisms and the possibility of two classes of radio emitting MCVs. Paper three of this survey will present high-resolution VLBI observations of MCVs, including the sources detected in this paper.

P.E.B. and P.A.M. acknowledge the guidance and inspiration of their late mentor and colleague G. Chanmugam, who began the search for radio emission from magnetic cataclysmic variables over 35 years ago. The National Radio Astronomy Observatory is a facility of the National Science Foundation operated under cooperative agreement by Associated Universities, Inc. This research has made use of the SIMBAD database, operated at CDS, Strasbourg, France ([Wenger et al. 2000](#)).

REFERENCES

- Bastian, T. S. 1987, PhD Thesis, Univ. Colorado
 Beasley, A. J., Bastian, T. S., Ball, L., & Wu, K. 1994, AJ, 108, 2207
 Bookbinder, J. A., & Lamb, D. Q. 1987, ApJ, 323, 131
 Chanmugam, G., & Wagner, R. L. 1978, ApJ, 222, 641
 Chanmugam, G., & Dulk, G. A. 1982, ApJ, 255, L107
 Chanmugam, G. 1987, Ap&SS, 130, 53
 Condon, J. J., Cotton, W. D., Fomalont, E. B., Kellermann, K. I., Miller, N., Perley, R. A., Scott, D., Vernstrom, T., & Wall, J. V. ApJ, 758, 23
 Coppejans, D. L., Körding, E. G., Miller-Jones, J. C. A., Rupen, M. P., Knigge, C., Sivakoff, G. R., & Groot, P. J. 2015, MNRAS, 451, 3801
 Coppejans, D. L., Körding, E. G., Miller-Jones, J. C. A., Rupen, M. P., Sivakoff, G. R., Knigge, C., Groot, P. J., Woudt, P. A., Waagen, E. O., & Templeton, M. 2016, MNRAS, 463, 2229
 Johns-Krull, C. M., & Valenti, J. A. 1996, ApJ, 459, L95
 Dulk, G. A., Bastian, T. S., & Chanmugam, G. 1983, ApJ, 273, 249
 Goldreich, P., & Lynden-Bell, D. 1969, ApJ, 156, 59
 Hjellming, R. M. & Wade, C. M. 1970, ApJL, 162, 1
 Mason, P. A., Fisher, P. L., & Chanmugam, G. 1996, A&A, 310, 132
 Mason, P. A. & Gray, C. L. 2007, ApJ, 600, 662
 Pavlin, P. E., Spencer, R. E., & Davis, R. J. 1994, MNRAS, 269, 779
 Rappaport, S., Verbunt, F., & Joss, P. C. 1983, ApJ, 275, 713
 Spruit, H. C. & Ritter, H. 1983, A&A, 124, 267
 Wenger, M., Ochsenbein, F., Egret, D., Dubois, P., Bonnarel, F., Borde, S., Genova, F., Jasniewicz, G., Laloë, S., Lesteven, S., & Monier, R. 2000, A&AS, 143, 9
 Wright, A. E., Cropper, M., Stewart, R. T., Nelson, G. J., & Slee, O. B. 1988, MNRAS, 231, 319